Catalysis Communications 20 (2012) 1–5 doi:10.1016/j.catcom.2011.12.039

(Short Communication)

Spectral response and stability of In_2S_3 as visible light-active photocatalyst

Raquel Lucena, Fernando Fresno, José C. Conesa*

Instituto de Catálisis y Petroleoquímica, CSIC

Campus de Excelencia UAM-CSIC

Marie Curie 2, Cantoblanco

28049 Madrid, Spain

Keywords: Photocatalysis, Visible light, Indium sulphide, Photocorrosion, Formic acid

Abstract

Nanocrystalline In_2S_3 is shown to degrade photocatalytically aqueous formic acid using visible light. Its spectral response for this process is verified for the first time, showing that even photons with ≈ 650 nm are active. In_2S_3 is also shown to be more active and photocorrosion resistant in this process than similarly prepared CdS.

1. Introduction

Photocatalysis with visible light is nowadays actively researched. Several semiconductors have been reported as photocatalysts able to use visible light: doped TiO_2 [1], binary oxides like WO_3, Bi_2O_3, Fe_2O_3 [2] or Cu_2O [3], mixed oxides like $BiVO_4$ [4] or $InTaO_4$ [5], (oxy)nitrides like Ta_3N_5 [6], $LaTiO_2N$ [7] or ZnO:GaN [8] and sulphides like CdS [9], Bi_2S_3 [10] or In_2S_3 [11,12]. Usually the activity with visible light is verified using a cut-off filter to block UV components from some wide spectrum source or testing a single wavelength (e.g. from a LED diode), without checking whether the spectral profile of the photocatalytic activity matches the absorption spectrum of the material.

This is verified here for In_2S_3, a semiconductor for which photocatalysis with visible light (i.e. excluding UV components) has been studied scarcely [11–13]. In its more common forms In_2S_3 has a spinel-type structure with cation vacancies. If these are disordered the structure appears cubic to XRD, being indexable in space group Fd-3m, and is called α-In_2S_3 [14]; in its most stable form the vacancies are located at tetrahedral sites and ordered so as to

produce a superstructure with tripled c axis and tetragonal symmetry (space group I41/amd), this is called β-In_2S_3 [15]. A less stable hexagonal form, ε-In_2S_3, is known [16]; besides, another hexagonal form γ-In_2S_3 can be stabilized by doping with As or Sb [17] and can also appear occasionally in the absence of such dopants [18]. In well crystallized form In_2S_3 has a direct bandgap of width E_g = 2.0 eV [19] and displays an orange or orange-brown colour; it may be noted that In_2S_3 prepared in aqueous environment, in particular when ill-crystallized or disordered (appearing thus as α phase), frequently contains oxygen in part of the anionic sites, which widens the gap and leads to a yellow colour.

As will be shown here, In_2S_3 is active in the whole wavelength range of its bandgap absorption, i.e. already the lowest energy photons that can excite electrons across its bandgap are able to drive a photocatalytic reaction. Its behaviour is compared also with that of CdS, a widely studied semiconductor having Eg ≈ 2.4 eV [20].

2. Experimental

In_2S_3 was synthesized hydrothermally from $InCl_3$ and thiourea at 463 K as reported in a previous work [18]; CdS was synthesized similarly from $Cd(CH3COO)_2.2H_2O$ (Aldrich 99.99+%) and thiourea in 1:4 molar ratio (which favours obtaining only the most stable phase having hexagonal wurtzite structure [21]) at 453 K during 48 h. Elemental compositions were checked with total reflection X-ray fluorescence. Specific surfaces were measured with N_2 at 77 K over samples pre-outgassed at 140 °C. X-ray diffractograms were collected using Cu Kα radiation (λ = 1.542 Å); from them lattice parameters were obtained by fitting to computed patterns using Powdercell pro- gram [22]. Diffuse reflectance UV-vis-NIR spectra were obtained using Spectralon® as reference.

Photocatalytic activity was measured in a thermostated, magnetically stirred suspension containing 40 mg of sulphide in 80 mL of aqueous HCOOH (1.5 mM), which unless stated otherwise was buffered to pH = 2.5 (to avoid any complications in kinetic data interpretation which might arise due to pH changes along the reaction) using a mixture of H_3PO_4 and NaH_2PO_4 in 1:1 molar proportion, and irradiated through a pyrex window using an ozone-free 450 W Xenon lamp provided with a water filter and, when so desired, a band-pass optical filter transmitting a wavelength interval of FWHM ≈ 50 nm. The light intensity incident on the liquid was measured with a radiometer.

1.5 mL of suspension was sampled periodically, filtered with a hydrophilic PTFE 0.45 µm filter and analysed for HCOOH in the liquid through its absorbance at λ = 205 nm. The eventual photocatalyst corrosion during reaction was checked by subsequently filtering the solid, washing it with doubly deionised water and analyzing with ICP-OES both metal and sulphur in the liquids obtained.

3. Results and discussion

3.1. Characterization of materials

The synthesized In_2S_3 (an orange powder) has a S:In ratio identical within 1% to the nominal 3:2 stoichiometry and specific surface SBET ≈ 40 m^2/g. Its diffractogram shows (Fig. 1a) the pattern of the In_2S_3 defect spinel (JCPDS 32–0456 card), all of its peaks being indexed accordingly; its measured fcc lattice constant is 10.734 Å, close to the reported value (10.774 Å [14]). It may be noted that, if the material contained the cation vacancies ordered as in the β phase, with consequent decrease of the symmetry to tetragonal, a diffraction peak corresponding to the (112) reflection should appear, according to the simulations, at 2θ ≈ 17.4º, with intensity similar to that at 2θ ≈ 23.4º; no such feature was observed. Indexing of the observed XRD peaks according to the tetragonal phase, which obviously is also possible, has been omitted in Fig. 1. For the synthesized CdS, which showed a S:Cd atomic ratio close to the theoretical one and a specific surface SBET =8 m^2/g, the XRD pattern (Fig. 2a), revealing a well crystallized material, can be explained on the basis of the sole presence of the hexagonal (wurtzite) phase, with lattice constants a = 4.134 Å and c = 6.751 Å (reported values: a = 4.132 Å, c = 6.734 Å [23]); the corresponding indexing is shown in Fig. 2a. The presence of the cubic CdS phase can be excluded since its characteristic (200) reflection at 2θ ≈ 30.7º is absent.

Fig. 1b displays the diffuse reflectance UV–vis-NIR spectrum of the In_2S_3 sample as Kubelka–Munk transform of the reflectance R (KM = (1 − R)2/2R [24]). Absorption starts at λ ≈ 600 nm; a Tauc plot of $(h\nu\alpha)^2$ vs. hν (see inset in Fig. 1b), as corresponds to the direct nature of its bandgap, yields Eg = 2.1 eV, close to the literature value. For CdS (Fig. 2b) the absorption edge starts at λ ≈ 525 nm; the Tauc plot (see inset in Fig. 2b) yields Eg = 2.4 eV, also in good agreement with the literature value.

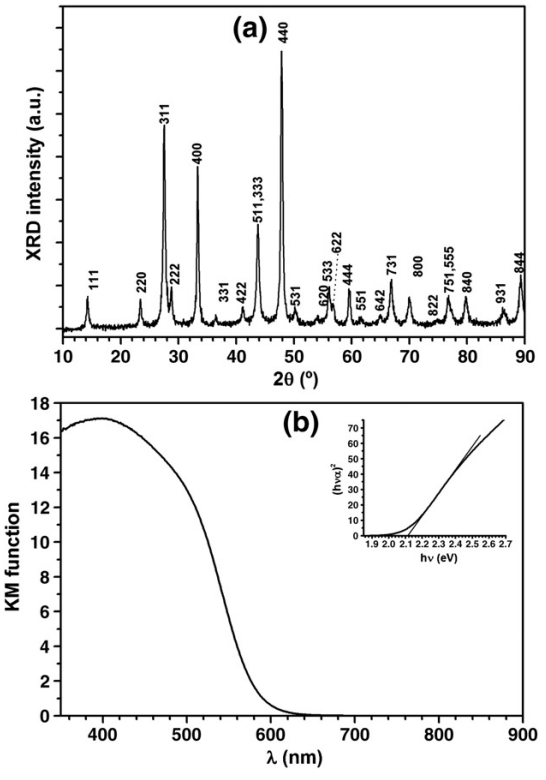

Fig. 1. Data for the hydrothermally synthesized In_2S_3: (a) Powder XRD diagram (with peak indexing corresponding to cubic In_2S_3) and (b) UV–VIS-NIR absorption spectrum (given as Kubelka–Munk transform of the diffuse reflectance); the inset displays the bandgap determination.

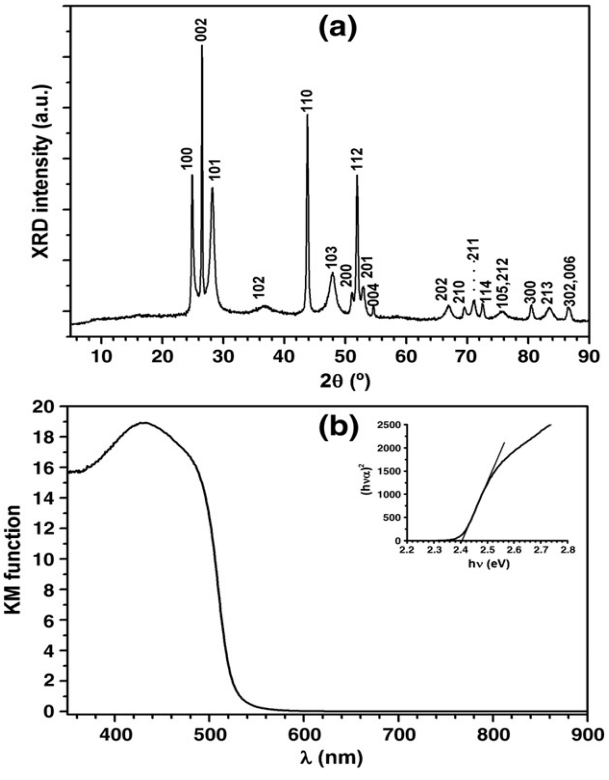

Fig. 2. Data for the hydrothermally synthesized CdS: (a) Powder XRD diagram (with peak indexing corresponding to hexagonal CdS) and (b) UV–VIS-NIR absorption spectrum (given as Kubelka–Munk transform of the diffuse reflectance); the inset displays the bandgap determination.

3.2. Photocatalytic activity tests

An In_2S_3 suspension in buffered aqueous HCOOH was first kept in the dark for 30 min to ensure a well equilibrated situation and in particular a stable HCOOH concentration (adsorption was anyway small: it was subsequently verified that only 1.2% of the dissolved amount was adsorbed) and was then irradiated with the unfiltered light of the Xenon lamp. In this setup the total light flux incident on the surface of the suspension was ≈ 115 mW/cm^2. HCOOH was quickly degraded as shown by the UV spectra of the extracted aliquots (Fig. 3a). Fig. 3b plots the concentration decay during irradiation; a quite similar decay profile was obtained in a test in which synthetic air was bubbled through the suspension during the experiment, showing that the magnetic stirring is quite enough to provide from ambient air the amount of oxygen needed for the reaction. The same figure shows also that no significant decay occurs in the dark; equally, no significant decay occurs in absence of In_2S_3 (data not shown). It may be added that in non-buffered solution (having also initially pH = 2.5) a similar decay occurs (data not shown) with effective rate constant k = 0.021 min^{-1}; the presence of phosphate has thus no major effect on the reaction rate. In this case the pH rose to 5 at the end of the process, which may be ascribed to the HCOOH concentration decrease.

The effective first-order rate constant determined from the initial slope was k = 0.018 min^{-1}. The assumed overall reaction is

$$HCOOH + ½\ O_2 \rightarrow CO_2 + H_2O \qquad (1)$$

The alternative process that would produce H_2 rather than consuming O_2:

$$HCOOH \rightarrow CO_2 + H_2 \qquad (2)$$

is not expected to occur here since previous work on photocatalysis with In_2S_3 using sacrificial reagents has shown that such H_2 evolution requires platinum or a similar co-catalyst to be present [14]. Also HCOOH dehydration to give CO and H_2O is unlikely here since this process normally requires a rather acidic catalyst, which is not the case for In_2S_3. A partial oxidation process to give oxalic acid and water can be excluded as well, at least as main reaction, since as said above in experiments carried out without buffer the pH rises to reach values close to 5.0, i.e. acidity is suppressed.

In process (1) O_2 molecules capture photogenerated electrons giving O_2^- and O_2H radicals (upon proton addition). This is expected to be quite possible in In_2S_3 since its CB position is rather high; according to literature its flatband potential is ≈−0.95 eV vs. SCE [25], i.e. about 0.7 V more negative than the normal H_2/H^+ electrode (in agreement with calculated values [26]). Both these radicals and the photogenerated holes may oxidize HCOOH either directly or via generation of intermediate OH radicals, although forming these latter directly from the VB holes might be more difficult for In_2S_3 than for other semiconductors since its VB edge is located very close to the $OH^{\cdot}/H_2O$ potential [26] and therefore the holes in it might not be oxidizing enough to form OH radicals. All radicals mentioned would anyway decompose ultimately giving the said products.

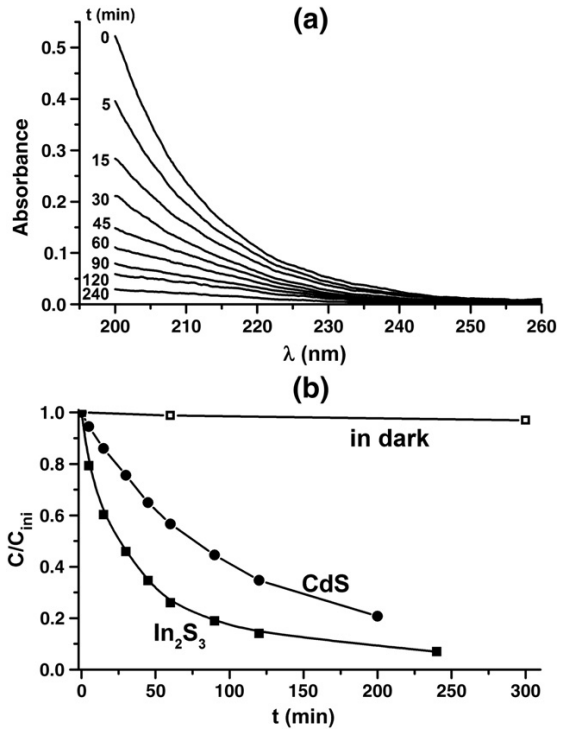

Fig. 3. (a) UV spectra of dissolved HCOOH taken at different times t after start of irradiation with full Xenon lamp light in a buffered suspension of In_2S_3. (b) Decay of the HCOOH concentration during irradiation of the suspension, measured from the absorbance at λ = 205 nm. The similar evolutions in the dark and under irradiation in a suspension of CdS are also displayed.

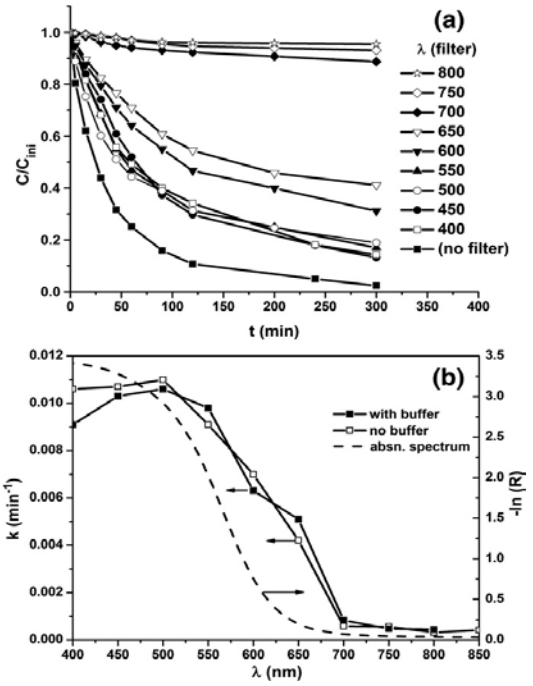

Fig. 4. (a) HCOOH concentration decay in a buffered aqueous suspension of In_2S_3, irradiated through bandpass filters of different wavelengths λ; the decay observed with unfiltered light is also shown. (b) Effective first-order rate constant k, measured from the initial slope of the decay curves obtained with the different filters in both buffered and unbuffered suspensions, compared with the Vis-NIR spectrum (given as negative logarithm of the diffuse reflectance R) of the In_2S_3 photocatalyst used.

The same experiment was made using CdS at the same concentrations (Fig. 3b), the corresponding (apparent) rate constant being k = 0.0088 min^{-1}. Thus In_2S_3 is significantly more active than the frequently used CdS. Since the measured position of the conduction band minimum of CdS in respect to redox couples in solution is lower than that of In_2S_3 by ca. 0.2 eV [26], the observed difference in photoactivity might be due to a slower electron transfer to O_2 in the CdS case.

The wavelength dependence of the photoactivity was checked for In_2S_3 using bandpass filters. Fig. 4a shows the decay observed for different values of λ (the nominal wavelength of the filter), each curve being obtained with a fresh photocatalyst portion. Fig. 4b plots the corresponding k values vs. λ. The action spectrum follows well the absorption profile of the material (once the filter transmission FWHM is taken into account); therefore one can conclude that all absorbed photon energies are active in the photoreaction. Since reactants and products absorb no visible or near-UV light, the photon-induced process must arise from light absorption in the solid, which is not always ensured when photo-oxidizing a visible light-absorbing dye as done in many photocatalysis studies. The filtered light intensity on the liquid surface, measured with the radiometer, is roughly constant (≈ 5 mW/cm^2) in the wavelength range used; from it an apparent quantum yield η ≈ 1.7% is computed for irradiation with λ = 400–500 nm. This spectral response remains unchanged in the absence of buffer, as shown also in Fig. 4b, indicating that phosphate does not interfere after all with the photoreaction.

3.3. Photostability tests

Sulphide photocatalysts lose frequently activity during reaction due to corrosion accompanied by dissolution of the solid; it is normally assumed that this is due to weakening of the S-metal bond at the surface when holes are trapped at the latter (transforming S_2^- ions into reactive S^- species) and/or to attack to S_2^- ions by strongly oxidizing O^- or OH radicals[2]. To check the extent of this phenomenon in our system, repeated photooxidation runs using the full unfiltered light of the lamp were made on one same In_2S_3 portion, which was irradiated in repeated 5 h runs in buffered HCOOH solution, the formic acid concentration being restored after each run by addition of pure compound to the solution. The results (Fig. 5a) show that after prolonged irradiation the photocatalyst remained highly active. In a similar experiment CdS suffered larger activity loss (graph not shown): the HCOOH fraction remaining after 5 h of irradiation increased from 21% in the first run to 47% in the fifth one. After these runs the samples were tested again for photoactivity with unfiltered light. For In_2S_3 the k value measured was k = 0.0144 min^{-1}, i.e. ≈ 21% lower than for the fresh sample; for CdS it was k = 0.0041 min^{-1}, evidencing a significantly higher decrease (53%). The structures of the samples after these runs were checked with XRD; the obtained diagrams only showed the initial sulphide phases, without hints of any oxide phase nor amorphous contribution. Of course one cannot exclude the elimination of some particularly active sites of the surface, nor a modification of the latter by e.g. adsorption of sulphate ions.

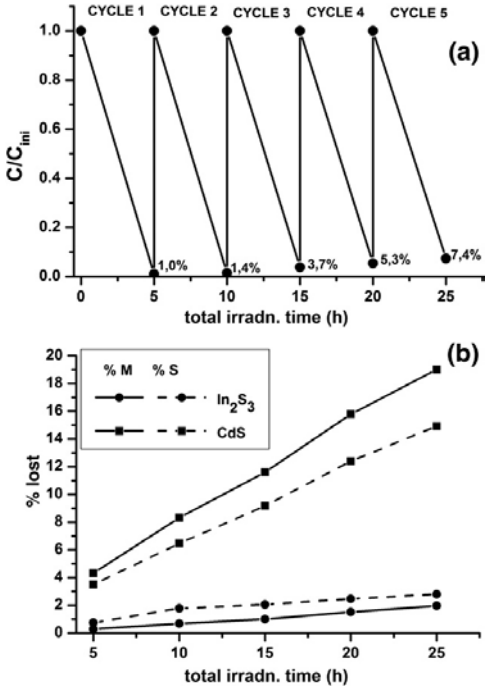

Fig. 5. (a) Extent of HCOOH concentration decay in five successive 5 h irradiation runs (adding fresh HCOOH at the start of each run) carried out with one same In_2S_3 portion in phosphate-buffered suspension. (b) Plot of the accumulated total amount of photo- catalyst constituents dissolved in five successive 5-h runs carried out with In_2S_3 or CdS on fresh HCOOH solutions, with intermediate separation of the solid. M% and S% represent the percentage of the total amount of metal and sulphur present in the initial solid specimen that become dissolved after the photoreaction runs.

In another experiment, after each 5-h run the solid was separated by centrifugation and the solution was analyzed, while the solid was added to a fresh HCOOH solution, the irradiation cycle being then repeated. Fig. 5b shows the accumulated amount of metal and sulphur gone into solution after each run, showing that In_2S_3 photocorrodes significantly less than CdS, in agreement with the previous observation that In_2S_3 retains photoactivity better than CdS. The amount of In_2S_3 dissolved in the dark was found to be much smaller, i.e. photon effect and not mere attack by the solution is the main factor in the observed corrosion. It is worth noting here that for CdS the corrosion was found to be noticeably lower (but still much larger than that of In_2S_3) with some earlier preparations of it having lower specific surfaces. This higher stability of In_2S_3 may be related to the sulphide lattice cohesion, probably higher in the denser In_2S_3 structure thanks to the higher charge and higher coordination of cations (75% of In is octahedral in

In_2S_3 while CdS has all Cd tetrahedral), which leads to larger Madelung cohesion energy.

These experiments also verify that the reaction is overall (photo) catalytic, not stoichiometric, in respect to the sulphide: for In_2S_3 ca. 0.6 mmol HCOOH are converted in the five 5-hour runs, while the sulphide used contains 0.29 mmol In, of which less than 2% gets dissolved. Photocorrosion is higher for CdS, but the argument about the (photo)catalytic character of the process still applies.

4. Conclusions

These results confirm that, as previously reported, In_2S_3 is an active photocatalyst for oxidizing organics in aqueous solution, and provide evidence, not given before, that the full range of photons absorbed by it (i.e. all those with energy above its ≈ 2.0 eV bandgap, which corresponds to λ = 620 nm) contributes to the process. In_2S_3 shows higher photocatalytic activity and resistance to photocorrosion than the frequently used CdS; this, together with the lower toxicity of In, makes In_2S_3 an attractive alternative to CdS for a range of photocatalytic applications.

Acknowledgements

This work was supported by projects GENESIS-FV (nr. CSD2006-0004) of the Consolider-Ingenio programme and FOTOMAT (nr. MAT2009-14625-C03) of the Plan Nacional de Materiales, both financed by the Spanish Plan Nacional de Investigación, and programme NUMANCIA-2 (nr. S2009ENE-1477) from the Comunidad de Madrid. R. L. thanks also CSIC for an I3P PhD grant.

References

[1] See e.g. several reviews in, M. Anpo, P.V. Kamat (Eds.), Environmentally Benign Catalysts - Applications of Titanium Oxide-Based Photocatalysts, Springer, New York, 2010. a) N. Serpone, A. V. Emeline, V. N. Kuznetsov, V. K. Ryabchuk, pp. 35–112. b) J. Zhou, X. S. Zhao, pp. 235–252. c) T. Ono, T. Tsubota, pp. 253–276. d) M. Fernández-Gar- cía, A. Martínez-Arias, J. C. Conesa, pp. 277–300. e) M. Takeuchi, M. Anpo, pp. 301–320.

[2] P. Maruthamuthu, K. Gurunathan, E. Subramanian, M. Ashokkumar, Bulletin of the Chemical Society of Japan 64 (1991) 1933.

[3] M. Hara, T. Kondo, M. Komoda, S. Ikeda, K. Shinohara, A. Tanaka, J.N. Kondo, K. Domen, Chemical Communications (1998) 357.

[4] A. Kudo, K. Ueda, H. Kato, I. Mikami, Catalysis Letters 53 (1998) 229.

[5] Z.G. Zou, J.H. Ye, H. Arakawa, Materials Research Bulletin 36 (2001) 1185.

[6] G. Hitoki, A. Ishikawa, T. Takata, J.N. Kondo, M. Hara, K. Domen, Chemistry Letters (2002) 736736.

[7] A. Kasahara, K. Nukumizu, T. Takata, J.N. Kondo, M. Hara, H. Kobayashi, K. Domen, The Journal of Physical Chemistry. B 107

(2003) 791.

[8] K. Maeda, K. Teramura, T. Takata, M. Hara, N. Saito, K. Toda, Y. Inoue, H. Kobayashi, K. Domen, The Journal of Physical Chemistry. B 109 (2005) 20504.

[9] T. Aruga, K. Domen, S. Naito, T. Onishi, K. Tamaru, Chemistry Letters (1983) 1037. [10] Y. Bessekhouad, M. Mohammedi, M. Trari, Solar Energy Materials and Solar Cells 73 (2002) 339.

[11] Y. He, D. Li, G. Xiao, W. Chen, Y. Chen, M. Sun, H. Huang, X. Fu, Journal of Physical Chemistry C 113 (2009) 5254.

[12] W. Wang, W. Zhu, L. Zhang, Research on Chemical Intermediates 35 (2009) 761. [13] X. Fu, X. Wang, Z. Chen, Z. Zhang, Z. Li, D.Y.C. Leung, L. Wu, X. Fu, Applied Catalysis B: Environmental 95 (2010) 393.

[14] C. Adenis, J. Olivier-Fourcade, J.C. Jumas, E. Philippot, Revue de Chimie Minérale 24 (1987) 10.

[15] G.A. Steigmann, H.H. Sutherland, J. Goodyear, Acta Crystallographica 19 (1965) 967.

[16] K.J. Range, M. Zabel, Zeitschrift für Naturforschung. Teil B 33 (1978) 463.

[17] R. Diehl, C.D. Carpentier, R. Nitsche, Acta Crystallographica. Section B 32 (1976) 1257.

[18] R. Lucena, I. Aguilera, P. Palacios, P. Wahnón, J.C. Conesa, Chemistry of Materials 20 (2008) 5125.

[19] K. Kambas, A. Anagnostopoulos, S. Ves, B. Ploss, J. Spyridelis, Physica Status Solidi (b) 127 (1985) 201.

[20] M. Cardona, M. Weinstein, G.A. Wolf, Physical Review 140 (1965) 633.

[21] N. Bao, L. Shen, T. Takata, K. Domen, A. Gupta, K. Yanagisawa, C.A. Grimes, Journal of Physical Chemistry C 111 (2007) 17527.

[22] Powdercell program v. 2.4, http://www.bam.de/de/service/publikationen/powder_cell.htm.

[23] M. Ikeda, H. Wada, T. Wada, T. Hirao, Journal of Crystal Growth 135 (1994) 476. [24] G. Dupuis, M. Menu, Applied Physics A: Materials Science and Processing 83 (2006) 469.

[25] J. Herrero, J. Ortega, Solar Energy Materials 17 (1988) 357.

[26] Y. Xu, M.A.A. Schoonen, American Mineralogist 85 (2000) 543.